Using Molecular Design to Control the Performance of Hydrogen-Producing Polymer-Brush-Modified Photocathodes

ARTICLE *in* JOURNAL OF PHYSICAL CHEMISTRY LETTERS · SEPTEMBER 2014

Impact Factor: 7.46

1 AUTHOR:

Gary F Moore

Arizona State University

46 PUBLICATIONS **695** CITATIONS

THE JOURNAL OF PHYSICAL CHEMISTRY Letters

Letter

pubs.acs.org/JPCL

Using Molecular Design to Control the Performance of Hydrogen-Producing Polymer-Brush-Modified Photocathodes

Diana Cedeno,[‡,¶] Alexandra Krawicz,[‡,¶] Peter Doak,[⊥,§] Min Yu,[§] Jeffrey B. Neaton,[§,#,□] and Gary F. Moore*[,†,▽]

[†]Physical Biosciences Division, [‡]Materials Science Division, [¶]Joint Center for Artificial Photosynthesis (JCAP), and [§]Molecular Foundry, Lawrence Berkeley National Laboratory, Berkeley, California 94720, United States

[⊥]Department of Chemistry and [#]Department of Physics, University of California, Berkeley, California 94720, United States

[□]Kavli Energy NanoSciences Institute at Berkeley, Berkeley, California 94720, United States

[▽]Department of Chemistry and Biochemistry, Arizona State University, Tempe, Arizona 85287-1604, United States

Supporting Information

ABSTRACT: Attachment of difluoroborylcobaloxime catalysts to a polymer-brush-modified GaP semiconductor allows improved hydrogen production levels and photoelectrochemical performance under aqueous acidic conditions (pH = 4.5) as compared to the performance of electrodes without catalyst treatment. The catalytic assembly used in this work incorporates a boron difluoride (BF_2) capping group on the glyoximate ligand of the catalyst, a synthetic modification previously used to enhance the stability of nonsurface-attached complexes toward acid hydrolysis and to shift the cobalt reduction potentials of the complex to less negative, and thus technologically more relevant, values. The pH-dependent photoresponses of the cobaloxime- and difluoroborylcobaloxime- modified semiconductors are shown to be consistent with those from analogous studies using non-surface-attached cobaloxime catalysts as well as catalysts supported on conductive electrodes. Thus, this work illustrates the potential to control and optimize the properties of visible-light-absorbing semiconductors using polymeric overcoating techniques coupled with the principles of synthetic molecular design.

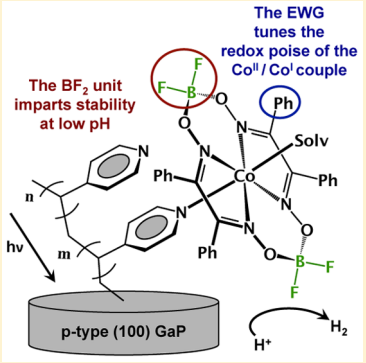

SECTION: Energy Conversion and Storage; Energy and Charge Transport

Energy conversion in photosynthesis offers a paradigm to develop technologies that harness, convert, and store solar energy.[1−4] However, a goal of artificial photosynthesis is to develop solar-to-fuels systems with efficiencies much greater than those of their biological counterparts.[5−8] Achieving this goal presents fundamental research and engineering challenges.[9,10] Fundamental research challenges include developing methods to effectively interface visible-light-absorbing units to multielectron, multiproton fuel catalysis using materials that are both manufacturably scalable and robust under operational conditions. However, the appropriate operating conditions of a solar fuel generator are currently unknown, and cases have been made for the advantages of operating in near-neutral pH as well as more caustic environments (i.e., basic and/or acidic conditions).[11−13] In addition, a majority of molecular fuel catalysts are initially designed and optimized for operation in solution, with the use of sacrificial chemical agents or an electrode providing the driving force,[14,15] and it is often uncertain how or if a given complex will function when immobilized at a surface. Further, in standard electrochemical measurements, changes in potential are used to alter the rate of electron transfer. These changes in potential at a metal/electrolyte interface appear across an electrical double layer (Helmholtz layer), changing the activation energy of the reaction and hence the rate of electron transfer. In contrast, changes in potential at a semiconductor/electrolyte interface appear mostly across the space charge region in the semiconductor and not across the Helmholtz layer.

Our investigations in the area of directly interfacing light capture and conversion technologies with catalysis have led us to develop a modular process to rapidly assemble promising combinations of semiconductors and catalysts.[16] Using this strategy, we can modify the choice of light absorber, linking material, or catalyst as new materials (or new uses for old ones) and discoveries emerge. In addition, we have previously reported[17] using polyvinylpyridine-modified p-type gallium phosphide[18−21] to assemble cobaloxime catalysts[14,22,23] for hydrogen production. The integrated photocathode (**1**) (Figure 1) is capable of photochemically producing hydrogen upon illumination in buffered as well as unbuffered solutions at neutral pH. We now show for the first time that incorporation of a cobaloxime with a ligand macrocycle that is modified at the molecular level affects the photoelectrochemical response to pH observed at the construct level.

Received: August 4, 2014
Accepted: September 2, 2014
Published: September 2, 2014

   dx.doi.org/10.1021/jz5016394 | J. Phys. Chem. Lett. 2014, 5, 3222−3226

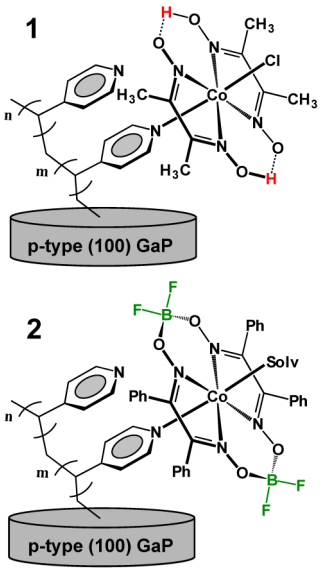

Figure 1. Schematic representations of cobaloxime-polymer-modified semiconductors containing (**1**) a H-bridged ligand as well as (**2**) a BF_2-bridged analogue.

Preparation of GaP wafers bearing surface-attached polyvinylpyridine has been described in a previous report.[17] In summary, buffered hydrofluoric acid etching of diced GaP wafers (~1 cm^2) is used to remove native surface oxide and provide hydroxyl-terminated surface sites (Figures S1 and S2, Supporting Information (SI)) for UV-induced surface grafting[24−29] and polymerization of the 4-vinylpyridine monomer. The resulting surface-attached polymer can be used as a scaffold for assembling cobaloxime catalysts at pyridyl sites. For the difluoroborylcobaloxime-modified cathode (**2**) used in this report, the oxime-linking hydrogen atoms of the cobalt-containing precursor, $Co(dphgH)_2(H_2O)_2$, are replaced with bridging BF_2 groups prior to assembly of the hybrid photocathode, yielding $Co(dphgBF_2)_2(H_2O)_2$ (see the SI Synthesis section). This synthetic manipulation has previously been used to impart stability during solution operation of cobaloxime catalysts in acidic conditions and to tune the catalytic redox features of cobaloximes to less negative values.[30,31]

Verification of the synthetic efforts used to assemble **2** is achieved using surface-sensitive spectroscopic methods, including X-ray photoelectron spectroscopy (XPS) and grazing angle attenuated total reflection Fourier transform infrared spectroscopy (GATR-FTIR). These methods provide converging evidence of successful attachment of difluoroborylcobaloximes to the PVP-functionalized semiconductor. Survey spectra of **2** show the presence C, N, O, F, B, and Co elements of the catalysts (Figure S3, SI). Further, Co 2p core-level region spectra (Figure 2a) show peaks centered at 780.4 ($2p_{3/2}$) and 795.6 eV ($2p_{1/2}$) (Table S1, SI) that are characteristic of the intact difluoroborylcobaloxime complex, $Co(dphgBF_2)PyH_2O$ (Figures S4 and S5, SI), including an observed 2:1 branching ratio with a multiplet splitting of 15.2 eV and a low-intensity satellite structure.[32,33] The measured elemental ratios of Co/B/F are Co/B = 1/1.9, Co/F =1/3.6, and B/F = 1/1.9. Further, core-level N 1s spectra of **2** show two spectral contributions centered at 399.9 and 398.7 assigned to nitrogens coordinated to the Co centers of attached catalysts, at higher binding energies, as well as pyridine units on the polymer chain that are not coordinated to Co, at lower binding energies. (Figure S9, SI).

GATR-FTIR spectra of **2** provide additional evidence of successful catalyst attachment. Figure 3 compares spectra of PVP-functionalized GaP, **1**, and **2**. As previously reported, the frequencies of the five absorption bands centered in the 1400−1600 cm^{-1} frequency range are assigned to C−N and C−H vibrations of the grafted polymer (Table S2, SI).[34] Upon attachment of catalysts to pyridyl sites on the polymer-modified GaP, forming constructs **1** or **2**, the spectrum is modified in this region, as explained below, and new peaks due to ligand vibration modes of the catalysts appear in the region below 1300 cm^{-1}. In addition, for constructs **1** and **2**, the reduction in relative intensity of the peak near 1602 cm^{-1}, associated with a pyridine ring mode, indicates coordination to the catalyst.

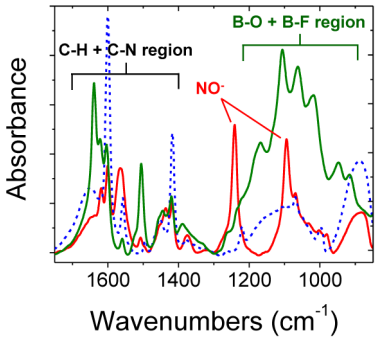

Figure 3. GATR-FTIR spectra of PVP-functionalized GaP (blue dash), construct **1** (red), and construct **2** (green).

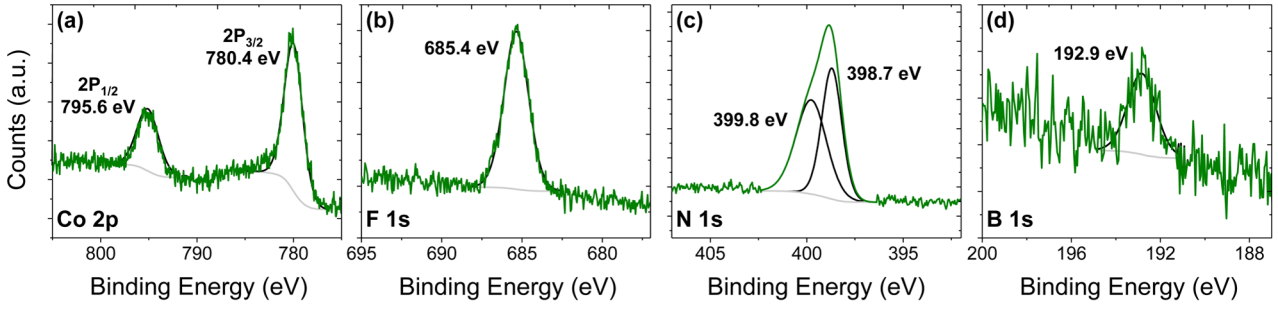

Figure 2. (a−d) Core-level XPS spectra including (a) Co 2p, (b) F 1s, (c) N 1s, and (d) B 1s regions of construct **2** (green). The gray and black lines represent the Shirley background and the component fits, respectively.

dx.doi.org/10.1021/jz5016394 | J. Phys. Chem. Lett. 2014, 5, 3222−3226

The improved understanding and control over the degrees of freedom and vibrational structure of catalytic units upon immobilization is likely a salient feature to improving the activity of surface-attached catalysts. To this end, we engaged in density functional theory (DFT) calculations, which are described in detail in the SI, of model systems relevant to this study, the isolated pyridine ligated version of constructs **1** and **2**, and the PVP dimer. As was previously stated, the vibrational spectra of PVP-functionalized GaP substrates before and after catalyst attachment reveal many changes in the 1400−1600 cm^{-1} region (Figure 3). Our calculations explain the appearance of peaks related to dphg C−N and phenyl C−H bend modes in this region, occurring most significantly in experiment (theory) at 1505 (1492 cm^{-1}) and ∼1450 cm^{-1} (1452 cm^{-1}) (Tables S2 and S3, SI). We note that the peak associated with the dphg ligand at ∼1450 cm^{-1} (1452 cm^{-1}) overlaps with an additional mode at 1453 cm^{-1} that is assigned to the CH_2 PVP backbone. Additionally, the unbound pyridyl ring mode peak at 1602 cm^{-1} (1590 cm^{-1}) (Table S5 and Figure S64, SI) in experiment (theory) is reduced in relative intensity as a result of its absence once pyridyl groups are bound as a ligand to Co (Figure S12, SI). In calculations of the isolated catalyst, a peak associated with the OH bend of Co-bound aqua ligands is found at 1576 cm^{-1}, which in combination with the experimental spectrum of Co-$(dphgBF_2)_2PyH_2O$ explains the broad peaks that appear in construct **2** at around 1600 cm^{-1}. In addition, spectra of **2** display intense absorption bands in the B−O and B−F stretching region (1200−800 cm^{-1})[35] and no observable features associated with the NO^- stretching mode (1240 cm^{-1}) (theory 1256 cm^{-1}) that is observed in **1**.

Attachment of the catalytic units to the polymer-modified GaP surface allows direct photoelectrochemical testing in aqueous environments under varying pH conditions. We note that the modified cathodes described in this report (**1** and **2**) are prepared from wafers cut from a different ingot of commercially obtained GaP, with different doping levels and physical properties (see the SI Materials section), as compared to those used in our previous reports.[17,36] Linear sweep voltammograms of **1** and **2**, measured at pH 7.0 (0.1 M phosphate buffer) and pH 4.5 (0.1 M acetate buffer), under simulated AM 1.5 illumination (100 mW cm^{-2}), are shown in Figure 4.

For construct **2**, a significantly increased photoactivity and near-quantitative production of hydrogen (Figure S20, SI), as compared to the performance of **1** or electrodes without catalyst treatment, is only observed at lower pH. These results indicate that proton activity at neutral pH is not high enough to boost hydrogen production upon illumination of **2** to the levels observed when using **1** (−0.56 mA cm^{-2} at 0 V versus RHE when using **2** as the working electrode versus −1.2 mA cm^{-2} at 0 V versus RHE when using **1**). Similar pH effects on catalytic performance have been noted in solution-based studies of (bis)dioxime cobalt complexes and their difluoroboryl analogues.[37] In these reports, requirement of a strong acid to induce catalysis is attributed to a correlation between the Co^{II}/Co^{I} reduction potential and the basicity of Co^{I} to form Co^{III} hydride during the catalytic cycle. For example, Eisenberg and co-workers have reported the use of cobaloxime catalysts in a photocatalytic system for H_2 generation from aqueous solutions of a Pt(II) terpyridyl acetylide chromophore and a sacrificial electron donor (triethanolamine).[38] $Co(dmgH)_2PyCl$ was shown to be an effective catalyst at pH 8.5, whereas the

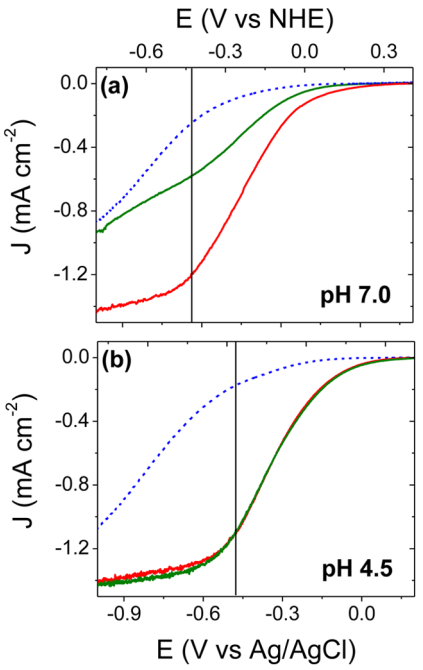

Figure 4. Linear sweep voltammograms of PVP-functionalized GaP (blue dash), **1** (red), and **2** (green) recorded at (a) pH 7 and (b) pH 4.5 under simulated AM 1.5 illumination. The vertical lines indicate 0 V versus RHE.

analogous difluoroborylated species is not. In their study, analysis at lower pH was complicated by the pK_a of the sacrificial electron donor used in these experiments. However, in an example of an immobilized electrocatalyst, Berben and Peters have reported a chemically modified electrode composed of $Co(dmgBF_2)_2(MeCN)_2$ adsorbed to glassy carbon that is active for hydrogen evolution in aqueous solutions below pH 4.5.[37]

Despite incorporation of the acid-stabilizing BF_2 units in **2**, the observed photocurrents do decrease with time. Figure S18 (SI) shows controlled potential electrolysis results obtained using working electrodes, composed of **1** or **2**, poised at −0.39 V versus NHE under simulated AM1.5 solar illumination. Under these conditions, electrodes **1** and **2** show a similar decrease in photocurrent with an average of 3 and 2% per minute, respectively. XPS analysis of the electrodes following exposure to electrolyte as well as photoelectrochemical testing (Figures S21 and S22, SI) shows that remaining cobalt complexes maintain electronic and structural integrity. In the Co 2p region, the two sets of signals corresponding to the $2p_{3/2}$ and $2p_{1/2}$ are still observed, and there are no detectable peaks below 780.9 eV corresponding to the presence of cobalt oxide or metallic cobalt.

Our results indicate that factors other than acid-induced hydrolysis of the dmgH or $dphgBF_2$ ligand of the catalysts contribute to the decrease in performance. While a detailed analysis of all possible degradation pathways is unavailable, detachment of cobalt centers from surface-grafted pyridines upon reduction from Co^{II} to Co^{I} is a likely point of failure. Previous computational and experimental work indicates that the axial pyridine of cobaloxime complexes can become labile during redox cycling.[39−41] However, using an innovative covalent attachment strategy that avoids binding though pyridyl moieties, Artero and co-workers have already shown that diimine−dioxime cobalt catalysts grafted to carbon nanotubes

dx.doi.org/10.1021/jz5016394 | J. Phys. Chem. Lett. 2014, 5, 3222−3226

are capable of robust electrocatalytic operation, achieving 55 000 turnovers in 7 h.[42]

As the molecular, electronic, and nanoscale properties that favor efficient photocatalytic performance and durability are identified, the modular nature of the approach used in this work, to directly couple catalysts to visible-light absorbers, should also allow modification of the attachment strategy. Although structural changes to the cobaloxime ligand environment can tune the redox potentials of catalysts to less negative values, large differences in photoperformance between photocathodes **1** and **2** are not apparent at pH 4.5 but are at pH 7. This result is rationalized in terms of the coupled nature of the chemical reaction catalyzed at the electrode surface (i.e., the formation of hydrogen involves the transfer of protons as well as electrons). Thus, the incorporation of electron-withdrawing groups on the ligand environment of the catalyst to favor transfer of electrons at less negative potentials also adversely affects the proton-transfer energetics. This highlights the promise of catalysts capable of decoupling the tuneability of the electron- and proton-transfer energetics by incorporating built-in positioned bases to deliver protons to a reactive metal site. Such features are captured in the hydrogenase inspired catalysts reported by DuBois and co-workers.[21,43−45] In these complexes, pendent amines provide relays that deliver substrate protons to a metal hydride stabilized by a soft bisdiphosphine ligation environment. However, effective attachment of catalysts that operate via more sophisticated mechanisms may also require improved immobilization strategies or the preparation of new catalysts specifically designed for operation when attached at a surface or immobilized within a confined environment. Although recent research efforts in this area[15,16,34,42,43,46] illustrate the promise of using immobilized molecular components in catalytic and photocatlytic materials, the development of effective attachment strategies and interfaces remains a major challenge.

In conclusion, GATR-FTIR and XPS confirm the successful attachment of a BF_2-capped cobaloxime hydrogen evolution catalyst to a polymer-modified semiconductor. The presence of difluoroborylcobaloximes significantly enhances photochemical performance of the GaP photocathode in aqueous conditions at low pH, compared to results obtained using GaP without catalyst functionalization. To the extent of our knowledge, this is the first time that the photoactivity and associated hydrogen production of a semiconductor are shown to be influenced by changes to the ligand environment of the molecular catalysts grafted at the semiconductor surface. This work illustrates the potential to control and optimize the properties of visible-light-absorbing semiconductors using polymeric overcoating techniques coupled with the principles of molecular design.

■ ASSOCIATED CONTENT

Ⓢ Supporting Information

Material descriptions, instrument descriptions, experimental details, computational details, XPS data, FTIR data, electrochemical and photoelectrochemical data, GC data, and computational results. This material is available free of charge via the Internet at http://pubs.acs.org.

■ AUTHOR INFORMATION

Corresponding Author

*E-mail: gfmoore@lbl.gov or gary.f.moore@asu.edu.

Author Contributions

The manuscript was written through contributions of all authors. All authors have given approval to the final version of the manuscript.

Notes

The authors declare no competing financial interest.

■ ACKNOWLEDGMENTS

The authors thank Dr. Yongjing Lin for his assistance with the external quantum efficiency measurement. This material is based upon work performed at the Joint Center for Artificial Photosynthesis, a DOE Energy Innovation Hub, supported through the Office of Science of the U.S. Department of Energy under Award Number DE-SC0004993 and at the Molecular Foundry supported by the Office of Science, Office of Basic Energy Sciences, of the U.S. Department of Energy under Contract No. DE-AC02-05CH1123. G.F.M. acknowledges support from the College of Liberal Arts and Sciences at Arizona State University.

■ REFERENCES

(1) Bolton, J. R.; Hall, D. O. Photochemical Conversion and Storage of Solar Energy. *Annu. Rev. Energy* **1979**, *4*, 353−401.
(2) Bard, A. J.; Fox, M. A. Artificial Photosynthesis: Solar Splitting of Water to Hydrogen and Oxygen. *Acc. Chem. Res.* **1995**, *28*, 141−145.
(3) Faunce, T.; Styring, S.; Wasielewski, M. R.; Brudvig, G. W.; Rutherford, A. W.; Messinger, J.; Lee, A. F.; Hill, C. L.; deGroot, H.; Fontecave, M.; et al. Artificial Photosynthesis as a Frontier Technology for Energy Sustainability. *Energy Environ. Sci.* **2013**, *6*, 1074−1076.
(4) Faunce, T. A.; Lubitz, W.; Rutherford, A. W.; MacFarlane, D.; Moore, G. F.; Yang, P.; Nocera, D. G.; Moore, T. A.; Gregory, D. H.; Fukuzumi, S.; et al. Energy and Environment Policy Case for a Global Project on Artificial Photosynthesis. *Energy Environ. Sci.* **2013**, *6*, 695−698.
(5) Blankenship, R. E.; Tiede, D. M.; Barber, J.; Brudvig, G. W.; Fleming, G.; Ghirardi, M.; Gunner, M. R.; Junge, W.; Kramer, D. M.; Melis, A.; et al. Comparing Photosynthetic and Photovoltaic Efficiencies and Recognizing the Potential for Improvement. *Science* **2011**, *332*, 805−809.
(6) Hammarström, L.; Winkler, J. R.; Gray, H. B.; Styring, S. Shedding Light on Solar Fuel Efficiencies. *Science* **2011**, *333*, 288.
(7) Tran, P. D.; Wong, L. H.; Barber, J.; Loo, J. S. C. Recent Advances in Hybrid Photocatalysts for Solar Fuel Production. *Energy Environ. Sci.* **2012**, *5*, 5902−5918.
(8) Swierk, J. R.; Mallouk, T. E. Design and Development of Photoanodes for Water-Splitting Dye-Sensitized Photoelectrochemical Cells. *Chem. Soc. Rev.* **2013**, *42*, 2357−2387.
(9) *Directing Matter and Energy: Five Challenges for Science and the Imagination*; U.S. Department of Energy: Washington, DC, 2007.
(10) *New Sciences for Secure and Sustainable Energy Future*; U.S. Department of Energy: Washington, DC, 2008.
(11) Hernandez-Pagan, E. A.; Vargas-Barbosa, N. M.; Wang, T. H.; Zhao, Y.; Smotkin, E. S.; Mallouk, T. E. Resistance and Polarization Losses in Aqueous Buffer-Membrane Electrolytes for Water-Splitting Photoelectrochemical Cells. *Energy Environ. Sci.* **2012**, *5*, 7582−7589.
(12) Jacobsson, T. J.; Fjaellstroem, V.; Sahlberg, M.; Edoff, M.; Edvinsson, T. A Monolithic Device for Solar Water Splitting Based on Series Interconnected Thin Film Absorbers Reaching over 10% Solar-to-Hydrogen Efficiency. *Energy Environ. Sci.* **2013**, *6*, 3676−3683.
(13) Modestino, M. A.; Walczak, K. A.; Berger, A.; Evans, C. M.; Haussener, S.; Koval, C.; Newman, J. S.; Ager, J. W.; Segalman, R. A. Robust Production of Purified H_2 in a Stable, Self-Regulating, and Continuously Operating Solar Fuel Generator. *Energy Environ. Sci.* **2014**, *7*, 297−301.
(14) Artero, V.; Chavarot-Kerlidou, M.; Fontecave, M. Splitting Water with Cobalt. *Angew. Chem., Int. Ed.* **2011**, *50*, 7238−7266.

(15) McKone, J. R.; Marinescu, S. C.; Brunschwig, B. S.; Winkler, J. R.; Gray, H. B. Earth-Abundant Hydrogen Evolution Electrocatalysts. *Chem. Sci.* **2014**, *5*, 865−878.
(16) Moore, G. F.; Sharp, I. D. A Noble-Metal-Free Hydrogen Evolution Catalyst Grafted to Visible Light-Absorbing Semiconductors. *J. Phys. Chem. Lett.* **2013**, *4*, 568−572.
(17) Krawicz, A.; Yang, J.; Anzenberg, E.; Yano, J.; Sharp, I. D.; Moore, G. F. Photofunctional Construct that Interfaces Molecular Cobalt-Based Catalysts for H_2 Production to a Visible-Light-Absorbing Semiconductor. *J. Am. Chem. Soc.* **2013**, *135*, 11861−11868.
(18) Bockris, J. O. M.; Uosaki, K. The Rate of the Photoelectrochemical Generation of Hydrogen at p-Type Semiconductors. *J. Electrochem. Soc.* **1977**, *124*, 1348−1355.
(19) Tomkiewicz, M.; Woodall, J. M. Photoassisted Electrolysis of Water by Visible Irradiation of a p-Type Gallium Phosphide Electrode. *Science* **1977**, *196*, 990−991.
(20) Grätzel, M. Photoelectrochemical Cells. *Nature* **2001**, *414*, 338−344.
(21) Kaiser, B.; Fertig, D.; Ziegler, J.; Klett, J.; Hoch, S.; Jaegermann, W. Solar Hydrogen Generation with Wide-Band-Gap Semiconductors: GaP(100) Photoelectrodes and Surface Modification. *ChemPhysChem* **2012**, *13*, 3053−3060.
(22) Dempsey, J. L.; Brunschwig, B. S.; Winkler, J. R.; Gray, H. B. Hydrogen Evolution Catalyzed by Cobaloximes. *Acc. Chem. Res.* **2009**, *42*, 1995−2004.
(23) Mulfort, K. L.; Mukherjee, A.; Kokhan, O.; Du, P.; Tiede, D. M. Structure−Function Analyses of Solar Fuels Catalysts Using In Situ X-ray Scattering. *Chem. Soc. Rev.* **2013**, *42*, 2215−2227.
(24) Cicero, R. L.; Linford, M. R.; Chidsey, C. E. D. Photoreactivity of Unsaturated Compounds with Hydrogen-Terminated Silicon(111). *Langmuir* **2000**, *16*, 5688−5695.
(25) Steenackers, M.; Kueller, A.; Stoycheva, S.; Grunze, M.; Jordan, R. Structured and Gradient Polymer Brushes from Biphenylthiol Self-Assembled Monolayers by Self-Initiated Photografting and Photopolymerization (SIPGP). *Langmuir* **2009**, *25*, 2225−2231.
(26) Richards, D.; Zemlyanov, D.; Ivanisevic, A. Assessment of the Passivation Capabilities of Two Different Covalent Chemical Modifications on GaP(100). *Langmuir* **2010**, *26*, 8141−8146.
(27) Wang, X.; Ruther, R. E.; Streifer, J. A.; Hamers, R. J. UV-Induced Grafting of Alkenes to Silicon Surfaces: Photoemission versus Excitons. *J. Am. Chem. Soc.* **2010**, *132*, 4048−4049.
(28) Chen, T.; Amin, I.; Jordan, R. Patterned Polymer Brushes. *Chem. Soc. Rev.* **2012**, *41*, 3280−3296.
(29) Moffitt, M. G. Self-Assembly of Polymer Brush-Functionalized Inorganic Nanoparticles: From Hairy Balls to Smart Molecular Mimics. *J. Phys. Chem. Lett.* **2013**, *4*, 3654−3666.
(30) Bakac, A.; Espenson, J. H. Unimolecular and Bimolecular Homolytic Reactions of Organochromium and Organocobalt Complexes. Kinetics and Equilibria. *J. Am. Chem. Soc.* **1984**, *106*, 5197−5202.
(31) Connolly, P.; Espenson, J. H. Cobalt-Catalyzed Evolution of Molecular Hydrogen. *Inorg. Chem.* **1986**, *25*, 2684−2688.
(32) Chuang, T. J.; Brundle, C. R.; Rice, D. W. Interpretation of the X-ray Photoemission Spectra of Cobalt Oxides and Cobalt Oxide Surfaces. *Surf. Sci.* **1976**, *59*, 413−429.
(33) Dillard, J. G.; Schenck, C. V.; Koppelman, M. H. Surface Chemistry of Cobalt in Calcined Cobalt-Kaolinite Materials. *Clays Clay Miner.* **1983**, *31*, 69−72.
(34) Panov, V. P.; Kazarin, L. A.; Dubrovin, V. I.; Gusev, V. V.; Kirsh, Y. E. Infrared Spectra of Atactic Poly(4-vinylpyridine). *Zh. Prikl. Spektrosk.* **1974**, *21*, 862−869.
(35) Cropek, D. M.; Metz, A.; Muller, A. M.; Gray, H. B.; Horne, T.; Horton, D. C.; Poluektov, O.; Tiede, D. M.; Weber, R. T.; Jarrett, W. L.; et al. A Novel Ruthenium(II)−Cobaloxime Supramolecular Complex for Photocatalytic H_2 Evolution: Synthesis, Characterisation and Mechanistic Studies. *Dalton Trans* **2012**, *41*, 13060−13073.
(36) Krawicz, A.; Cedeno, D.; Moore, G. F. Energetics and Efficiency Analysis of a Cobaloxime-Modified Semiconductor under Simulated Air Mass 1.5 Illumination. *Phys. Chem. Chem. Phys.* **2014**, *16*, 15818−15824.
(37) Berben, L. A.; Peters, J. C. Hydrogen Evolution by Cobalt Tetraimine Catalysts Adsorbed on Electrode Surfaces. *Chem. Commun.* **2010**, *46*, 398−400.
(38) Du, P.; Knowles, K.; Eisenberg, R. A Homogeneous System for the Photogeneration of Hydrogen from Water Based on a Platinum(II) Terpyridyl Acetylide Chromophore and a Molecular Cobalt Catalyst. *J. Am. Chem. Soc.* **2008**, *130*, 12576−12577.
(39) Muckerman, J. T.; Fujita, E. Theoretical Studies of the Mechanism of Catalytic Hydrogen Production by a Cobaloxime. *Chem. Commun.* **2011**, *47*, 12456−12458.
(40) Solis, B. H.; Hammes-Schiffer, S. Theoretical Analysis of Mechanistic Pathways for Hydrogen Evolution Catalyzed by Cobaloximes. *Inorg. Chem.* **2011**, *50*, 11252−11262.
(41) Veldkamp, B. S.; Han, W.-S.; Dyar, S. M.; Eaton, S. W.; Ratner, M. A.; Wasielewski, M. R. Photoinitiated Multi-step Charge Separation and Ultrafast Charge Transfer Induced Dissociation in a Pyridyl-Linked Photosensitizer−Cobaloxime Assembly. *Energy Environ. Sci.* **2013**, *6*, 1917−1928.
(42) Andreiadis, E. S.; Jacques, P.-A.; Tran, P. D.; Leyris, A.; Chavarot-Kerlidou, M.; Jousselme, B.; Matheron, M.; Pecaut, J.; Palacin, S.; Fontecave, M.; et al. Molecular Engineering of a Cobalt-Based Electrocatalytic Nanomaterial for Hydrogen Evolution under Fully Aqueous Conditions. *Nat. Chem.* **2013**, *5*, 48−53.
(43) Le, G. A.; Artero, V.; Jousselme, B.; Tran, P. D.; Guillet, N.; Metaye, R.; Fihri, A.; Palacin, S.; Fontecave, M. From Hydrogenases to Noble Metal-Free Catalytic Nanomaterials for H_2 Production and Uptake. *Science* **2009**, *326*, 1384−1387.
(44) Helm, M. L.; Stewart, M. P.; Bullock, R. M.; DuBois, M. R.; DuBois, D. L. A Synthetic Nickel Electrocatalyst with a Turnover Frequency above 100,000 s^{-1} for H_2 Production. *Science* **2011**, *333*, 863−866.
(45) Yang, J. Y.; Bullock, R. M.; DuBois, M. R.; DuBois, D. L. Fast and Efficient Molecular Electrocatalysts for H_2 Production: Using Hydrogenase Enzymes as Guides. *MRS Bull.* **2011**, *36*, 39−47.
(46) Tran, P. D.; Le Goff, A.; Heidkamp, J.; Jousselme, B.; Guillet, N.; Palacin, S.; Dau, H.; Fontecave, M.; Artero, V. Noncovalent Modification of Carbon Nanotubes with Pyrene-Functionalized Nickel Complexes: Carbon Monoxide Tolerant Catalysts for Hydrogen Evolution and Uptake. *Angew. Chem., Int. Ed.* **2011**, *50*, 1371−1374.